Parameter Estimation of Rheological Object Based on FE Simulation and Nonlinear Optimization

Zhongkui Wang and Shinichi Hirai
Department of Robotics, Ritsumeikan University
Noji-higashi 1-1-1, Kusatsu, Shiga 525-8577, Japan

***Abstract*—There are many kinds of deformable objects in our living life. Some of them demonstrate rheological behaviors, such as human tissues, food, and clay. Comparing with elastic or viscoelastic objects, rheological objects have not been studied intensively. Especially, effective methods for parameter identification have not been established until now. In this paper, we summarize two FE dynamic models associated with three-element and four-element physical model respectively. According to the analysis of simulation results, we proposed an approach for estimating physical parameters of rheological objects based on FE simulation and nonlinear optimization. This method aims at minimizing the difference of deformed shape and force response between experiment and simulation. This method take both deformed shape and force response into consideration. Experiment is conducted by using commercial clay. The identification results show that the four-element physical model is more appropriate to describe rheological behaviors than three-element model.**

I. Introduction

There are many kinds of deformable objects in our living life, such as human tissues, cloth, food, clay, and so on. The modeling and simulation of such objects have been studied since late 80's. Many applications have been involved in virtual reality, from previous applications for imitating dynamic behaviors of various deformable objects [1], [2], to current popular surgical applications for modeling and simulating of human tissues or organs [3]–[6], and also some other applications related with robot hand grasping [7], [8] and food engineering [9], [10]. If we can say that previous applications mostly focused on the visual approximation, then current applications are focusing on the haptic approximation, i.e., we want to make the simulation not only looks like the real deformation, but also feels like the real one.

So far, most related works of modeling and simulation of soft objects focus on elastic or viscoelastic objects (see Fig. 1c) because most living tissues and organs demonstrate elastic behaviors. On the contrary, the rheological objects (see Fig. 1e), as a combination of elastic and plastic objects, have not been given enough attention. In general, modeling a rheology object is more difficult than doing an elastic or viscoelastic object because the rheological object always leaves a residual deformation after pushing operation and we cannot understand how to control the residual displacement [11], [12]. So, the dynamic modeling of rheological deformation has not been well developed. Especially, the effective methods for estimating the physical parameters have not been established until now. The main contributions of our works concentrate on the modeling and parameter identification of rheological objects.

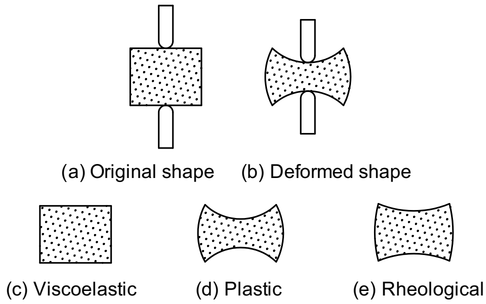

Fig. 1. The definitions of soft objects

The remainder of this paper is organized as follows: after giving the FE dynamic models associated with three-element and four-element physical model respectively in Section 2. We propose the parameter identification method in Section 3. Some experiments and identification results are given in Section 4. In Section 5, we will conclude this paper and suggest future works.

II. FE Dynamic Models

Depending on the deformation behaviors, soft objects can be roughly divided into three categories: viscoelastic, plastic, and rheological objects. Supposing that an object has a natural shape, as shown in Fig. 1(a). Applying external force, the object deformed as shown in Fig. 1(b). After removing the force, viscoelastic objects totally turn back to the original shape, as shown in Fig. 1(c). Plastic objects maintain all the deformation and there is no recovered deformation, as shown in Fig. 1(d). However, rheological objects partially maintain the deformation but not all, as shown in Fig. 1(e). Until now, two popular physical models used to describe rheological behaviors are three-element model (see Fig. 2(a)) and four-element model (see Fig. 2(b)).

In this section, we give the FE dynamic models based on these two physical models, respectively. Let us imagine that there is a rheological object with a size of $80\,\mathrm{mm}\times 80\,\mathrm{mm}\times 12.5\,\mathrm{mm}$. The bottom surface is fixed on the ground. From time $0\,\mathrm{s}$ to $20\,\mathrm{s}$, we push the object from top surface with a constant velocity of $0.5\,\mathrm{mm/s}$ and we call this time period push-phase. Before releasing the external force, we keep the deformation from time $20\,\mathrm{s}$ to $60\,\mathrm{s}$ and we call it keep-phase. Besides, through this paper, we use keep-shape and final-shape to denote the deformed shape in the end of keep-

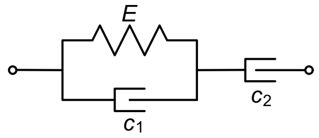

(a) Three-element physical model

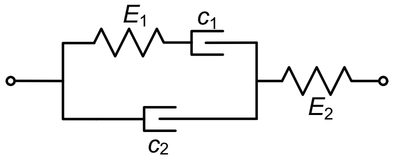

(b) Four-element physical model

Fig. 2. Popular physical models for describing rheological behaviors.

phase and the deformed shape after releasing, respectively. We suppose that this is 2D deformation and the object is described by a set of triangles. A three-element (see Fig. 2(a)) or four-element physical model (see Fig. 2(b)) is attached on each triangle. Since these two FE models have already presented in our previous works [13], [14], we just give the dynamic models directly in this paper and readers can check our previous works for detail information.

A. FE Model Based on Three-Element Physical Model

Let $\mathbf{u}_N$ be a set of displacements of nodal points. Let $\mathbf{J}_\lambda$ and $\mathbf{J}_\mu$ be connection matrices, which denote the connection configuration among triangles and can be geometrically determined by object coordinate components of nodal points. Let $\mathbf{M}$ be an inertia matrix and vector $\mathbf{f}$ be a set of external forces applied to nodal points. Let us describe a set of geometric constraints imposed on the nodal points by $\mathbf{A}^T\mathbf{u}_N = \mathbf{b}$, where $\mathbf{b}$ is a displacement vector of the constraints and matrix $\mathbf{A}$ decides which points are going to be constrained. Let vector λ be the Lagrange multipliers which denotes a set of constraint forces corresponding to the geometric constraints. Then, a set of dynamic equations of rheological deformation based on three-element physical model can be described as:

$$\begin{aligned}
\dot{\mathbf{u}}_N &= \mathbf{v}_N, \\
\mathbf{M}\dot{\mathbf{v}}_N - \mathbf{A}\lambda &= -\mathbf{J}_\lambda\omega_\lambda - \mathbf{J}_\mu\omega_\mu + \mathbf{f}, \\
-\mathbf{A}^T\dot{\mathbf{v}}_N &= \mathbf{A}^T(2\omega\mathbf{v}_N + \omega^2\mathbf{u}_N), \\
-\frac{\lambda_1^{vis}\lambda_2^{vis}}{\lambda_1^{vis}+\lambda_2^{vis}}\dot{\mathbf{v}}_N + \dot{\omega}_\lambda &= -\frac{\lambda^{ela}}{\lambda_1^{vis}+\lambda_2^{vis}}(\omega_\lambda - \lambda_2^{vis}\mathbf{v}_N), \\
-\frac{\mu_1^{vis}\mu_2^{vis}}{\mu_1^{vis}+\mu_2^{vis}}\dot{\mathbf{v}}_N + \dot{\omega}_\mu &= -\frac{\mu^{ela}}{\mu_1^{vis}+\mu_2^{vis}}(\omega_\mu - \mu_2^{vis}\mathbf{v}_N),
\end{aligned} \tag{1}$$

where λ^{ela}, λ_1^{vis}, λ_2^{vis}, μ^{ela}, μ_1^{vis}, and μ_2^{vis} can be calculated by four unknown physical parameters as follows:

$$\begin{aligned}
\lambda^{ela} &= \frac{E\gamma}{(1+\gamma)(1-2\gamma)}, & \mu^{ela} &= \frac{E}{2(1+\gamma)}, \\
\lambda_1^{vis} &= \frac{c_1\gamma}{(1+\gamma)(1-2\gamma)}, & \mu_1^{vis} &= \frac{c_1}{2(1+\gamma)}, \\
\lambda_2^{vis} &= \frac{c_2\gamma}{(1+\gamma)(1-2\gamma)}, & \mu_2^{vis} &= \frac{c_2}{2(1+\gamma)}.
\end{aligned} \tag{2}$$

A set of rheological forces applied to all nodal points are then simply described as:

$$\mathbf{F}^{rheo} = \mathbf{J}_\lambda\omega_\lambda + \mathbf{J}_\mu\omega_\mu. \tag{3}$$

B. FE Model Based on Four-Element Physical Model

Similarly, a set of dynamic equations of rheological deformation based on four-element physical model can be described as below:

$$\begin{aligned}
\dot{\mathbf{u}}_N &= \mathbf{v}_N, \\
\mathbf{M}\dot{\mathbf{v}}_N - \mathbf{A}\lambda &= -\mathbf{J}_\lambda(\omega_1^\lambda - \omega_2^\lambda) - \mathbf{J}_\mu(\omega_1^\mu - \omega_2^\mu) + \mathbf{f}, \\
-\mathbf{A}^T\dot{\mathbf{v}}_N &= \mathbf{A}^T(2\omega\mathbf{v}_N + \omega^2\mathbf{u}_N), \\
-\frac{B_1^\lambda}{m-n}\dot{\mathbf{v}}_N + \dot{\omega}_1^\lambda &= -n\omega_1^\lambda + \frac{B_0^\lambda}{m-n}\mathbf{v}_N, \\
-\frac{B_1^\mu}{m-n}\dot{\mathbf{v}}_N + \dot{\omega}_1^\mu &= -n\omega_1^\mu + \frac{B_0^\mu}{m-n}\mathbf{v}_N, \\
-\frac{B_1^\lambda}{m-n}\dot{\mathbf{v}}_N + \dot{\omega}_2^\lambda &= -m\omega_2^\lambda + \frac{B_0^\lambda}{m-n}\mathbf{v}_N, \\
-\frac{B_1^\mu}{m-n}\dot{\mathbf{v}}_N + \dot{\omega}_2^\mu &= -m\omega_2^\mu + \frac{B_0^\mu}{m-n}\mathbf{v}_N.
\end{aligned} \tag{4}$$

The detailed calculations of variables B_0^λ, B_1^λ, B_0^μ, B_1^μ, m, and n can be found in [14]. Then, a set of rheological forces based on four-element physical model can be formulated as:

$$\mathbf{F}^{rheo} = \mathbf{J}_\lambda(\omega_1^\lambda - \omega_2^\lambda) + \mathbf{J}_\mu(\omega_1^\mu - \omega_2^\mu). \tag{5}$$

III. Parameter Identification

The most popular method for estimating parameters of soft objects is optimization: the simulation is iterated with updated physical parameters until the difference between the simulation and experiment is minimized, as shown in Fig. 3. Many related works are using this idea to estimate parameters of soft objects. Unfortunately, most of them are only focus on minimizing the difference of deformed shapes. Along with the development of computer graphic and haptic sensing, we are eager to know how the force response will be during the deformation of soft objects. In this paper, we take both deformed shape and force response into consideration to yield a method to improve the accuracy of force approximation. At first, we use four-element

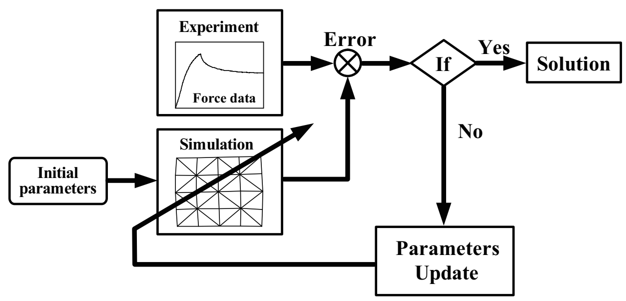

Fig. 3. Optimization process for parameter identification.

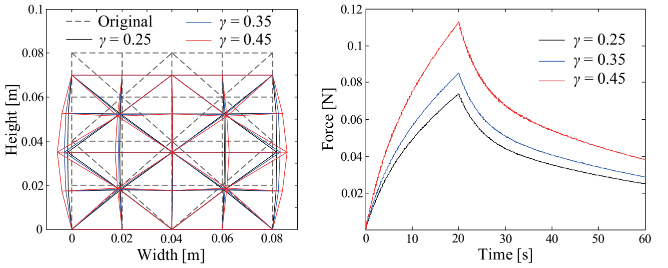

(a) Deformation behavior (b) Force response

Fig. 4. Comparison results of deformation behaviors with different Poisson's ratio γ.

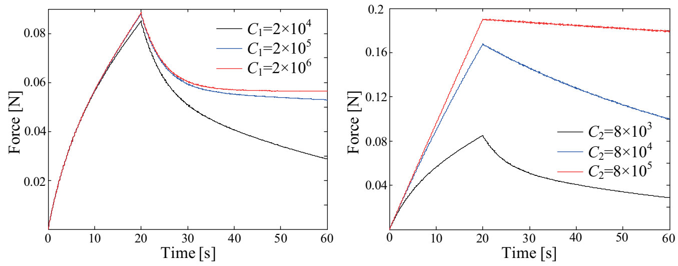

(a) Force response with different c_1 (b) Force response with different c_2

Fig. 6. Comparison results of deformation behaviors with different viscous moduli c_1 and c_2.

model as an example to investigate how these physical parameters affect the simulation results. Recall that the deformation behaviors of four-element model are decided by 5 physical parameters: E_1, E_2, c_1, c_2, and γ. But the contributions of these parameters are different to the consequential deformation and force response.

1) Contribution of Poisson's Ratio: Let us consider simulations with different Poisson's ratios: $\gamma = 0.25$, $\gamma = 0.35$, and $\gamma = 0.45$. Other four parameters are unchanged with values of $E_1 = 5 \times 10^2$ Pa, $E_2 = 1.2 \times 10^3$ Pa, $c_1 = 2 \times 10^4$ Pa·s, and $c_2 = 8 \times 10^3$ Pa·s. The comparison of keep-shape and force response are shown in Fig. 4. We can see that the Poisson's ratio γ affects both keep-shape and force response.

2) Contribution of Elastic Modulus: Let us compare simulation results with different elastic moduli. Fig. 5 shows the deformation behaviors with different E_1 and E_2. We can see that elastic moduli only contribute to force response, they do not affect the keep-shape at all.

3) Contribution of Viscous Modulus: Let us perform the same comparisons with different viscous moduli, as shown in Fig. 6. We only give the force responses with different c_1 and c_2 because the keep-shapes are same with Fig. 5. Fig. 6 indicates that the viscous moduli also only affect force responses.

In addition, mesh distribution also affects simulation results. A rule of thumb is that the finer the mesh is distributed, the higher the accuracy of simulation results will be. Fig. 7 shows how the mesh distributions affect simulation results. According to Fig. 7, we find that the discrepancy of both deformed shape and force response between different mesh distributions is not significant if the mesh distribution is finer than 4×4 in this simple deformation. So we employ 4×4 triangle mesh through our identification process.

According to the above simulation analysis, we find that only Poisson's ratio γ affect the keep-shape and other parameters have no contribution to this shape. This phenomenon suggests that we can identify Poisson's ratio γ separately by optimizing the keep-shape. So we divided our identification method into two steps. In the first step, we identify the Poisson's ratio γ by minimizing the keep-shape and we call this step as shape optimization. In the second step, the other parameters will be identified based on the optimization of force response and we call this step as force optimization. Both shape and force optimization process can be described by Fig. 3. The objective functions for both cases can be generalized as

$$F(x) = \sum_{i=1}^{m} \left[\omega f_i^{sim}(x) - \omega f_i^{exp}(x)\right]^2, \tag{6}$$

where x is the physical parameters. ω is a weight coefficient which is set to 1000 and 1 for shape and force optimization

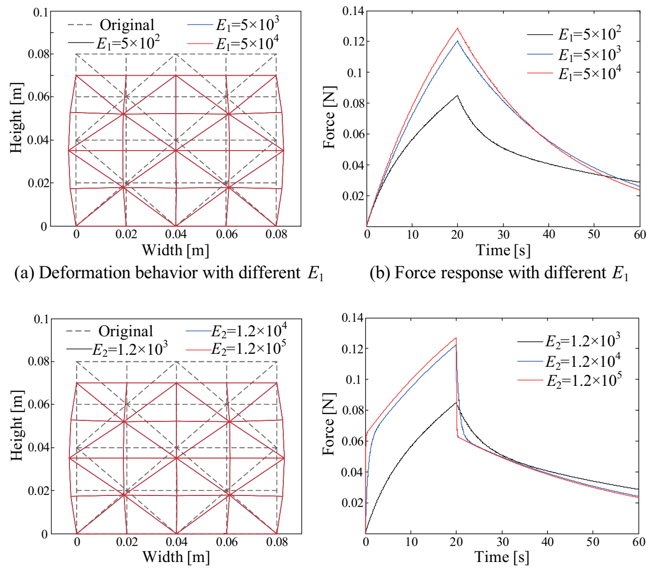

(a) Deformation behavior with different E_1 (b) Force response with different E_1

(c) Deformation behavior with different E_2 (d) Force response with different E_2

Fig. 5. Comparison results of deformation behaviors with different elastic moduli E_1 and E_2.

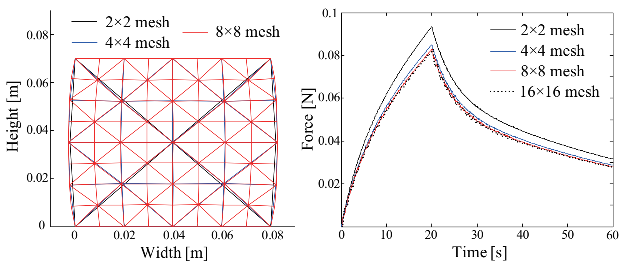

(a) Deformation Behavior (b) Force response

Fig. 7. Comparison results of deformation behaviors with different mesh distributions.

respectively. Vectors $f_i^{sim}(x)$ and $f_i^{exp}(x)$ are simulation and experiment data respectively. For shape optimization, $f_i^{sim}(x)$ and $f_i^{exp}(x)$ denote displacements of nodal points. For force optimization, they denote force response at every sampling time. Number m denotes how many nodal points are involved in shape optimization and how many times the forces are sampled in force optimization respectively.

In both optimizations, we employ optimization toolbox of Matlab software and 'Nonlinear Least Squares' method to minimize the objective functions. This method is widely used in data fitting problems.

IV. Experiment Results

The commercial clay made of flour, water, and salt was employed to work as a rheological object through our experiment. The object of size about $80\,\text{mm}\times 80\,\text{mm}\times 12.5\,\text{mm}$ was pushed by a motorized stage with a displacement about $9.6\,\text{mm}$ and a constant velocity of $0.5\,\text{mm/s}$. Before releasing, the displacement was kept about 47.88 seconds. Some markers were drawn on the surface of the clay by using a resist pen filled with lacquer ink. The initial and deformed shapes recorded by a camera are shown in Fig. 8(a), (b), and (c). By using a simple image processing, we can obtain 2D FE mesh of these shapes as shown in Fig. 8(d), (e), and (f). The force response on the bottom surface was recorded by a tactile sensor.

A. Identification Results for Three-Element Physical Model

1) Step 1: In the first step, we give some random values to other three parameters and iterate simulations with update Poisson's ratio γ until termination conditions stop the optimization process. For the three-element physical model, the random values for the other three parameters are given as: $E = 700\,\text{Pa}$, $c_1 = 500\,\text{Pa·s}$, and $c_2 = 1000\,\text{Pa·s}$. In addition, we set two termination conditions to stop the optimization. One is the changing of objective function value. Another one is the changing of identified parameter value. Both conditions are set as 1×10^{-6}. Table I gives the identification results of Poisson's ratio γ with different initial values. We can see that the identified Poisson's ratios in all trials are very similar with each other. This means we obtain the global minimum for this optimization problem. We use $\gamma = 0.3409$ for second step of three-element physical model.

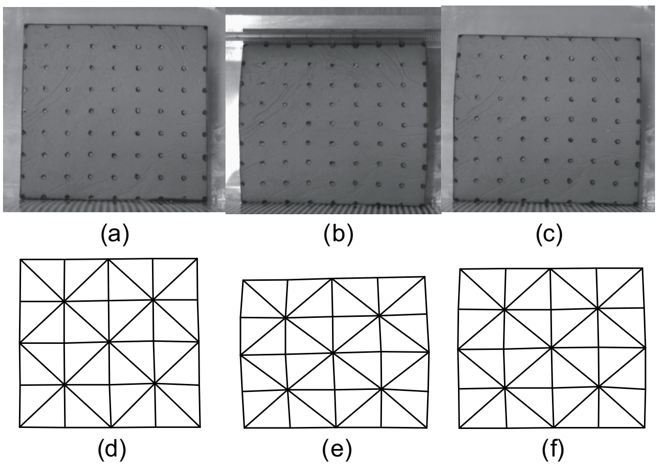

Fig. 8. Deformed shapes in experiment. (a), (b), (c): Images taken by camera. (d), (e), (f): Description by 2D triangle mesh. (a), (d): Initial shape. (b), (e): Keep-shape. (c), (f): Final-shape.

TABLE I
Identification Results of Poisson's Ratio γ for Three-Element Physical Model.

Trial no.	**Initial value x_0**	**Identified value x^***	$F(x)$ (mm^2)	**Iter. no.**
1	0.15	0.3408785	3.6062343	4
2	0.25	0.3408817	3.6062343	4
3	0.35	0.3408849	3.6062343	3
4	0.45	0.3408844	3.6062343	5

TABLE II
Identification Results of Parameters E, c_1, and c_2 for Three-Element Physical Model.

Para.	**Initial value x_0**	**Identified value x^***	$F(x)$ (N^2)	**Iter. no.**
E (Pa)	4×10^4	5.4939×10^4	15.6030	28
c_1 (Pa·s)	5×10^4	2.2814×10^5		
c_2 (Pa·s)	6×10^6	7.1967×10^6		

TABLE III
Identification Results of Poisson's Ratio γ for Four-Element Physical Model.

Trial no.	**Initial value x_0**	**Identified value x^***	$F(x)$ (mm^2)	**Iter. no.**
1	0.15	0.341160	3.605885	5
2	0.25	0.341145	3.605885	4
3	0.35	0.341149	3.605885	4
4	0.45	0.341156	3.605885	5

2) Step 2: After having Poisson's ratio γ, we can identify the other three parameters E, c_1, and c_2 by optimizing the force differences between experiment and simulation. Identification results are given in Table II.

B. Identification Results for Four-Element Physical Model

1) Step 1: Same with three-element physical model, we estimate the Poisson's ratio γ for four-element model in the first step. The random values for the other four parameters are given as: $E_1 = 500\,\text{Pa}$, $E_2 = 1000\,\text{Pa}$, $c_1 = 20000\,\text{Pa·s}$, and $c_2 = 8000\,\text{Pa·s}$. Then, the identification results for parameter γ with different initial values are given in Table III. We still can find the global minimum for parameter γ. We use $\gamma = 0.3412$ for the second step.

2) Step 2: Once again, in the second step. We identify all the other four parameters E_1, E_2, c_1, and c_2 by optimizing the force difference. We conduct two identification trials with different

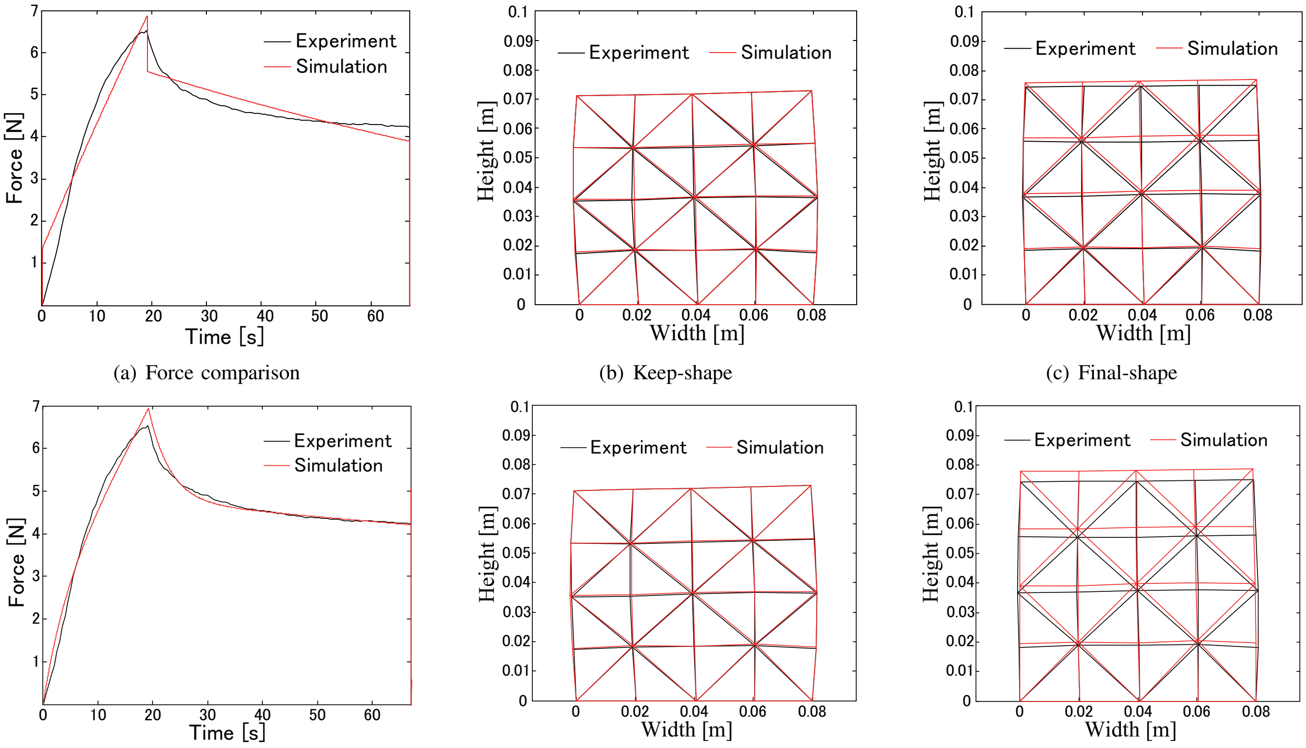

(a) Force comparison (b) Keep-shape (c) Final-shape

(d) Force comparison (e) Keep-shape (f) Final-shape

Fig. 9. Comparison results for both physical models. The first row denotes the comparison results of three-element model, the second row denotes the results from four-element model.

TABLE IV
IDENTIFICATION RESULTS OF PARAMETERS E_1, E_2, c_1 AND c_2 FOR FOUR-ELEMENT PHYSICAL MODEL.

Trial no.	**Para.**	**Initial value** x_0	**Identified value** x^*	$F(x)$ (N^2)	**Iter. no.**
trial 1	E_1 (Pa)	3×10^4	5.8525×10^4	3.8652	52
	E_2 (Pa)	5×10^3	1.2348×10^5		
	c_1 (Pa·s)	2×10^5	2.0556×10^7		
	c_2 (Pa·s)	6×10^5	8.3340×10^5		
trial 2	E_1 (Pa)	6×10^4	5.8481×10^4	3.6981	28
	E_2 (Pa)	2×10^5	1.3497×10^5		
	c_1 (Pa·s)	2×10^7	1.5845×10^7		
	c_2 (Pa·s)	1×10^6	7.4853×10^5		

initial values. The identification results are given in Table IV. We can see that identified parameters are slightly different with different initial values. This means we have several local minimums instead of one global minimum. Fortunately, we can choose one set of better solutions for these parameters according to the $F(x)$ values. Here we choose the identified parameters of trial 2.

After having all these parameters, we can finally simulate the rheological behaviors and compare with experiment results. The comparison results for both three-element model and four-element model are shown in Fig. 9. Comparing two rows of Fig. 9, we can see that we can obtain much better results for force approximation by using four-element physical model than three-element model. This is because that the force expression of four-element model include two exponential functions, but three-element model only has one. This coincide with our previous work [15] which shows that we need at least two exponential functions to obtain a good force approximation in the keep-phase for rheological deformation. From Fig. 9, we also find that the keep-shape approximation for both cases are quite good. On the contrary, the final-shape approximation for four-element model is worse than three-element model. This is because that we focus on the keep-shape and force response during our identification process and we did not take final-shape into consideration.

V. CONCLUSIONS AND FUTURE WORKS

In this paper, we compare the performance of two physical models for describing rheological objects. The first model is three-element physical model and the second one is four-element model. We give FE dynamic equations for both physical models. Then, we propose an approach to identify physical parameters based on FE simulation and nonlinear optimization. This identification method can be divided into 2 steps. In the first step, the Poisson's ratio is identified by minimizing the difference of keep-shape between experiment and simulation. In the second step, the other parameters are identified by optimizing the force differences. Experiment is conducted by using commercial clay. Identification results for both three-element and four-element physical models are given. The comparison results of deformed shapes and force responses show that the four-element physical model is more appropriate than three-element physical model to describe rheological behaviors.

In the future, the identification method will be used in non-uniform objects, for instance, an object consists of two or three layers with different parameters. On the other hand, the nonlinear behavior will be taking into account to develop more accurate model for rheological objects.

References

[1] D. Terzopoulos, J. Platt, A. Barr, and K. Fleischer, "Elastically Deformable Models," *Proc. 14th Annual Conference on Computer Graphics and Interactive Techniques (SIGGRAPH '87)*, vol.21, no.4, pp. 205-214, Jul. 1987.

[2] D. Terzopoulos and K. Fleischer,"Modeling Inelatic Deformation: Viscoelasticity, Plasticity, Fracture," *Proc. 15th Annual Conference on Computer Graphics and Interactive Techniques (SIGGRAPH '88)*, vol.22, no.4, pp. 269-278, Aug. 1988.

[3] M. Bro-Nielsen, "Finite Element Modeling in Surgery Simulation," *Proceedings of the IEEE*, vol.86, no.3, pp. 490-503, Mar. 1998.

[4] S. Cotin, H. Delingette, and N. Ayache, "Real-Time Elastic Deformations of Soft Tissues for Surgery Simulation," *IEEE Trans. Visualization and Computer Graphics*, vol.5, no.1, pp. 62-73, Jan/Mar. 1999.

[5] R. Balaniuk and K. Salisbury, "Soft-Tissue Simulation Using the Radial Elements Method," *Surgery Simulation and Soft Tissue Modeling*, vol.2673, pp. 48-58, Jan. 2003.

[6] G. Picinbono, H. Delingette, and N. Ayache, "Nonlinear and Anisotropic Elastic Soft Tissue Models for Medical Simulation," *Proc. IEEE International Conference on Robotics and Automation (ICRA '01)*, pp. 1370-1375, May. 2001.

[7] R. Brockett, "Robotic Hands with Rheological Surfaces," *Proc. IEEE International Conference on Robotics and Automation (ICRA '85)*, vol.2, pp. 942-946, Mar. 1985.

[8] T. Inoue and S. Hirai, "Elastic Model of Deformable Fingertip for Soft-Fingered Manipulation," *IEEE Trans. Robotics*, vol.22, no.6, pp. 1273-1279, Dec. 2006.

[9] S. Tokumoto, Y. Fujita, and S. Hirai, "Deformation Modeling of Viscoelastic Objects for Their Shape Control," *Proc. IEEE International Conference on Robotics and Automation (ICRA '99)*, vol. 1, pp. 767-772, May. 1999.

[10] M. Kimura, Y. Sugiyama, S. Tomokuni, and S. Hirai, "Constructing Rheologically Deformable Virtual Objects," *Proc. IEEE International Conference on Robotics and Automation (ICRA '03)*, vol.3, pp. 3737-3743, Sept. 2003.

[11] R. Nogami, H. Noborio, F. Ujibe, and H. Fujii, "Precise Deformation of Rheologic Object under MSD Models with Many Voxels and Calibrating Parameters," *Proc. IEEE International Conference on Robotics and Automation (ICRA '04)*, vol. 2, pp. 1919-1926, Apr/May. 2004.

[12] T. Ikawa and H. Noborio, "On the Precision and Efficiency of Hierarchical Rheology MSD Model," *Proc. IEEE/RSJ International Conference on Intelligent Robots and Systems (IROS '07)*, pp. 376-383, Oct/Nov. 2007.

[13] Z. Wang, K. Namima, and S. Hirai, "Physical Parameter Identification of Rheological Object Based on Measurement of Deformation and Force," *Proc. IEEE International Conference on Robotics and Automation (ICRA '09)*, pp. 1238-1243, May. 2009.

[14] Z. Wang and S. Hirai, "Modeling and Parameter Identification of Rheological Object Based on FE Method and Nonlinear Optimization," *Proc. IEEE/RSJ International Conference on Intelligent Robots and Systems (IROS '09)*, Oct. 2009, preprint.

[15] Z. Wang and S. Hirai, "Physical Parameter Identification of Rheological Object Based on FE Dynamic Model," *The Fourth Joint Workshop on Machine Perception and Robotics*, Beijing, Nov. 2008.